

# A Time-Varying Modified MMSE Detector for Multirate CDMA Signals in Fast Rayleigh Fading Channels

Kilsoo Jeong, Mitsuo Yokoyama, and Hideyuki Uehara

**In this paper, we propose a time-varying modified minimum mean-squared error (MMSE) detector for the detection of higher data rate signals in a multirate asynchronous code-division multiple-access (CDMA) system which is signaled in a fast Rayleigh fading channel. The interference viewed by a higher data rate symbol will be periodic due to the presence of a lower data rate symbol which spans multiple higher data rate symbols. The detection is carried out on the basis of a modified MMSE criterion which incorporates differential detection and the ratio of channel coefficients in two consecutive observation intervals inherently compensating the fast variation of the channel due to fading. The numerical results obtained by the MMSE detector with time-varying detection show around 3 dB ( $M=2$ ) and 6 dB ( $M=4$ ) performance improvement at a BER of  $10^{-3}$  in the AWGN channel, while introducing more computational complexity than the MMSE detector without time-varying detection. At a higher  $E_b/N_0$ , the proposed scheme can achieve a BER of approximately  $10^{-3}$  in the presence of fast channel variation which is an improvement over other schemes.**

**Keywords:** Time-varying modified MMSE detector, multirate asynchronous CDMA, fast fading channel.

## I. Introduction

In wireless communication systems, much effort has been devoted to offering heterogeneous kinds of traffic, such as voice, data, and video, which have different data rates and varying requirements for quality of service [1], [2]. To accommodate multiple data rates in code-division multiple-access (CDMA) systems, different multirate schemes have been proposed [3], [4]. Among the many alternatives proposed for multirate CDMA, we focus on the variable spreading length (VSL) system in this paper. In the VSL system, all users employ signature waveforms with the same chip rate, and the data rate is tied to the length of the spreading code of each user. One potential problem of VSL systems is that for a high-rate user, the cross correlations between different users' spreading sequences change from symbol to symbol, making it difficult to implement the adaptive minimum mean-squared error (MMSE) detector. To deal with this problem, MMSE detectors using cyclostationarity properties of the multirate CDMA system have been recently proposed [5], [6]. However, the authors of these papers assumed a static channel, that is, the channel coefficients were essentially fixed over the observation duration. Since this assumption is generally not true for mobile wireless communication systems, these adaptive algorithms are known to break down in the presence of fast channel variation, which is typical of a wireless channel.

If the channel coefficient is difficult to estimate, differential detection can be used for demodulation. Several MMSE detectors using differential detection have been proposed and evaluated. A multishot adaptive MMSE detector [7] incorporated with differential detection was proposed to remove fast phase variations in the desired user's signal due to fading, and a one-shot MMSE detector [8] incorporating

---

Manuscript received June 22, 2006; revised Jan. 05, 2007.

This work was partially supported as part of the the 21st Century COE program "Intelligent Human Sensing," by the Ministry of Education, Culture, Sports, Science, and Technology of Japan and NTT DoCoMo Inc.

Kilsoo Jeong (phone: +81 532 44 6761, email: ksjjeong@comm.ics.tut.ac.jp), Mitsuo Yokoyama (email: yokoyama@ics.tut.ac.jp), and Hideyuki Uehara (email: uehara@ics.tut.ac.jp) are with the Department of Information and Computer Science, Toyohashi University of Technology, Japan.

differential detection and amplitude compensation was proposed to achieve performance improvement with less computational complexity in a single-rate CDMA system. In [9], under the assumption that the channel coefficients in two consecutive observation intervals are approximately the same, an adaptive interference suppression detector based on the differential MMSE (DMMSE) criterion was presented for a single-rate CDMA system in rapidly time-varying channels. The common idea behind these schemes is to avoid the requirement for explicit channel estimation of the desired user in fast fading channels.

In this paper, we propose a new adaptive interference cancellation scheme based on the modified MMSE criterion which incorporates differential detection and the ratio of the channel coefficients in two consecutive observation intervals. This can inherently compensate for fast variations of the channel, thus the proposed adaptive detector has the ability to remove the multiple-access interference (MAI) and to provide immunity to the near-far problem in fast Rayleigh fading channels.

The rest of this paper is organized as follows. Section II describes an asynchronous dual-rate CDMA system wherein users are allowed to transmit with one of two different data rates in fast Rayleigh fading channels. We introduce a modified adaptive MMSE detector and we analyze the modified MMSE criterion in section III. In section IV, we introduce several differential-detection-based adaptive MMSE detectors which are used as benchmarks for evaluation of the proposed scheme, and we discuss the computational complexity. We study the performance of various systems by examining simulation results in section V. Finally, conclusions are made in section VI.

We define notations as follows: matrices are denoted by boldface upper case letters, and vectors are denoted by boldface lower case letters; superscripts  $(\cdot)^T$ ,  $(\cdot)^*$ , and  $(\cdot)^H$  denote the transpose, conjugate, and Hermitian transpose, respectively;  $E\{\cdot\}$  denotes the statistical expectation;  $\|\cdot\|$  denotes the Euclidian norm; and  $|\cdot|$  denotes the absolute values.

## II. System Description

We consider a dual-rate asynchronous CDMA system. The ratio between high-rate and low-rate is  $M$  such that  $T_s^{(l)} = MT_s^{(h)}$ , and  $T_s^{(l)}$  is the symbol duration such that the superscripts  $(l)$  and  $(h)$  refer to low-rate (LR) and high-rate (HR) users respectively. Figure 1 illustrates the block diagram of a dual-rate CDMA baseband system model with  $K (=K^{(h)}+K^{(l)})$  users. The received baseband signal model can be written as

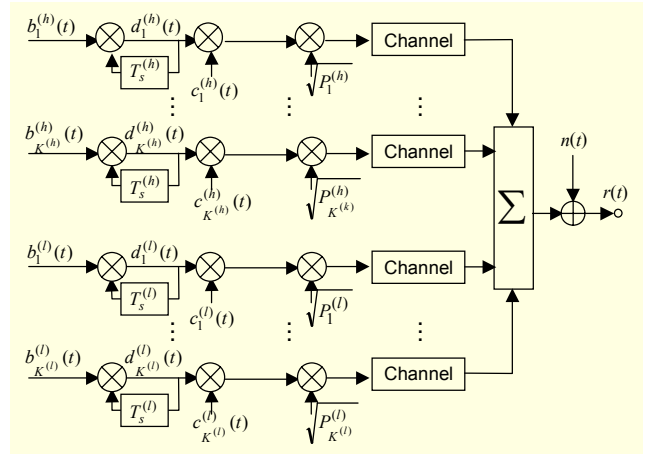


Fig. 1. Block diagram of a dual-rate CDMA baseband system model with  $K (=K^{(h)}+K^{(l)})$  users.

$$r(t) = \sum_{i=-\infty}^{+\infty} \left\{ \sum_{k=1}^{K^{(h)}} \sqrt{P_k^{(h)}} \alpha_k^{(h)}(t) d_k^{(h)}(t) \times c_k^{(h)}(t - \tau_k^{(h)} - iT_s^{(h)}) + \sum_{k=1}^{K^{(l)}} \sqrt{P_k^{(l)}} \alpha_k^{(l)}(t) d_k^{(l)}(t) \times c_k^{(l)}(t - \tau_k^{(l)} - iT_s^{(l)}) \right\} + n(t), \quad (1)$$

where we adopt the notations used in [5], as follows:  $K^{(l)}$  is the number of users,  $P_k^{(l)}$  represents the signal power,  $\alpha_k^{(l)}(t)$  is the complex channel coefficient,  $\tau_k^{(l)} \in [0, T_s^{(l)}]$  and  $c_k^{(l)}(t)$  are the delay and the signature waveform for the  $k$ -th user of each rate,  $d_k^{(l)}(t)$  represents the differentially encoded symbols of the information signal  $b_k^{(l)}(t)$ , and  $n(t)$  is the additive white Gaussian noise (AWGN) with zero mean and variance  $N_0/2$ .

In the VSL system, both HR and LR users share the same chip rate, thus the users with different data rates are assigned spreading sequences with variable length. For the VSL system, we have

$$c_k^{(h)}(t) = \sum_{n=0}^{N^{(h)}-1} s_{k,n}^{(h)} p_{T_c}(t - nT_c), \\ c_k^{(l)}(t) = \sum_{n=0}^{N^{(l)}-1} s_{k,n}^{(l)} p_{T_c}(t - nT_c), \quad (2)$$

where  $\{s_{k,n}^{(l)}\}_{n=0}^{N^{(l)}-1}$  is the spreading sequence assigned to the  $k$ -th user and

$$p_{T_c}(t) = \begin{cases} 1, & \text{for } t \in [0, T_c] \\ 0, & \text{otherwise,} \end{cases} \quad (3)$$

where  $T_c$  is the chip duration, and the spreading gain is  $N^{(l)} = T_s^{(l)}/T_c$ .

In the remainder of this paper, it will be assumed that the desired user is the first HR user, the power of the desired user is  $P_1^{(h)} = 1$ , and the detector is synchronized to the desired user's

signal, that is,  $\tau_i^{(h)} = 0$ . After chip matched filtering and chip rate sampling, we obtain the following  $N^{(h)} \times 1$  dimensional sequence:

$$\begin{aligned} r(i) &= \sqrt{P_1^{(h)}} \alpha_1^{(h)}(i) d_1^{(h)}(i) \mathbf{c}_1^{(h)} + \sum_{k=2}^{K^{(h)}} \sqrt{P_k^{(h)}} \alpha_k^{(h)}(i) d_k^{(h)}(i) \tilde{\mathbf{c}}_k^{(h)} \\ &\quad + \sum_{k=1}^{K^{(l)}} \sqrt{P_k^{(l)}} \alpha_k^{(l)}(i) d_k^{(l)}(i) \tilde{\mathbf{c}}_k^{(l)}(m) + \mathbf{n}(i) \\ &= \sqrt{P_1^{(h)}} \alpha_1^{(h)}(i) d_1^{(h)}(i) \mathbf{c}_1^{(h)} + \mathbf{u}(i) + \mathbf{n}(i), \end{aligned} \quad (4)$$

where the first term on the right-hand side represents the contribution from the desired user, while the second and third terms represent the MAI and noise contributions, respectively. The normalized spreading sequence of the  $k$ -th user is  $\mathbf{c}_k^{(l)} = (c_{k,0}^{(l)}, \dots, c_{k,N^{(l)}-1}^{(l)})^T$ , where  $\mathbf{c}_k^{(l)T} \mathbf{c}_k^{(l)} = 1$ ,  $\tilde{\mathbf{c}}_k^{(h)}$  is the  $k$ -th HR user's effective spreading code [8],  $\tilde{\mathbf{c}}_k^{(l)}(m)$  is the  $m$ -th segment of the  $k$ -th LR user's effective spreading code when  $m = i \bmod M$  (see Fig. 2).

It is assumed that the amplitude  $a_k^{(l)}(i)$  and the phase  $\phi_k^{(l)}(i)$  of the channel coefficient  $\alpha_k^{(l)}(i) = a_k^{(l)}(i) \exp(j\phi_k^{(l)}(i))$  are taken to be constant over the duration of a bit, even for fast Rayleigh fading environments. The channel is modeled as a Rayleigh fading channel [16], thus the channel coefficients for different users are independent, namely,  $\alpha_k^{(l)}(i)$  is independent of  $\alpha_j^{(l)}(n)$  for  $k \neq j$  and all  $i, n$ .

The interference covariance matrix  $\mathbf{R}_u(i) = E\{\mathbf{u}(i)\mathbf{u}^H(i)\}$  is periodically time-varying with period  $M$  [5]. Thus, time-varying detection is applied to accommodate the periodic interference viewed by the HR users due to an LR user whose data symbol and corresponding interference spans over multiple HR symbols.

### III. Time-Varying Modified MMSE Detector in the Presence of Fast Channel Variation

Figure 2 shows an example of the relationship between the dual-rate system and the tap weight vector for detecting the desired user when  $m = i \bmod M = 0$ . The original dual-rate signal can be equivalently converted to a single-rate signal through the equivalent synchronous representation of the LR user's signal and the time-varying MMSE detector  $\mathbf{x}(m)$  with period  $M$ . In this paper,  $\mathbf{x}(m)$  indicates the tap weight vector of the  $m$ -th segment of the time-varying MMSE detector with period  $M$ , and its instantaneous estimate for the  $i$ -th bit is represented as  $\mathbf{x}(i, m)$ .

In general, the periodically time-varying MMSE detector  $\mathbf{x}(m)$  for detecting the desired user's information bit  $d_1^{(h)}(i)$  when  $m = i \bmod M$  minimizes the mean square error (MSE)  $E\{d_1^{(h)}(i) - \mathbf{x}^H(i, m)\mathbf{r}(i)\}^2$  can be found as given in [5] and [10] as

$$\mathbf{x}(m) = \mathbf{R}^{-1}(i)\mathbf{p}(i), \quad (5)$$

where the covariance matrix  $\mathbf{R}(i)$  is given as

$$\mathbf{R}(i) = E\{\mathbf{r}(i)\mathbf{r}^H(i)\}, \quad (6)$$

and

$$\mathbf{p}(i) = E\{d_1^{(h)}(i)\mathbf{r}(i)\} \quad (7)$$

is the cross-correlation between  $d_1^{(h)}(i)$  and  $\mathbf{r}(i)$ .

For a fast Rayleigh fading channel in (4), under the assumptions that the bitstreams of different users are independent,  $d_1^{(h)}(i)$  is uncorrelated with  $d_k^{(h)}(i)$  for  $k \neq 1$ , and  $d_k^{(l)}(i)$  and  $\alpha_k^{(l)}(i)$  for all  $k$ . Thus, we obtain

$$\mathbf{p}(i) = E\{|d_1^{(h)}(i)|^2\} E\{\alpha_1^{(h)}(i)\} \mathbf{c}_1^{(h)} = E\{\alpha_1^{(h)}(i)\} \mathbf{c}_1^{(h)} = \mathbf{0}. \quad (8)$$

This results in  $\mathbf{x}(m) = \mathbf{0}$ . Thus, it is to be expected that the MMSE detector does not work well in a fast Rayleigh fading channel since the MMSE detector requires the channel coefficients to be constant over a sufficiently long interval. In many wireless communication applications, the channel is such that even when a spectral model is available, there are unknown and randomly time-varying parameters in the model. If the pilot symbols are used to track the channel and perform coherent demodulation, the transmission efficiency is reduced due to the insertion of the pilot symbol. This approach has been considered in [11] and [12]. In this paper, we focus on MMSE detectors incorporated with differential phase-shift keying (DPSK) modulation (as, for example, [7] and [8]) and we define the demodulated symbol as  $b_1^{(h)}(i) = d_1^{(h)}(i) d_1^{(h)}(i-1)$

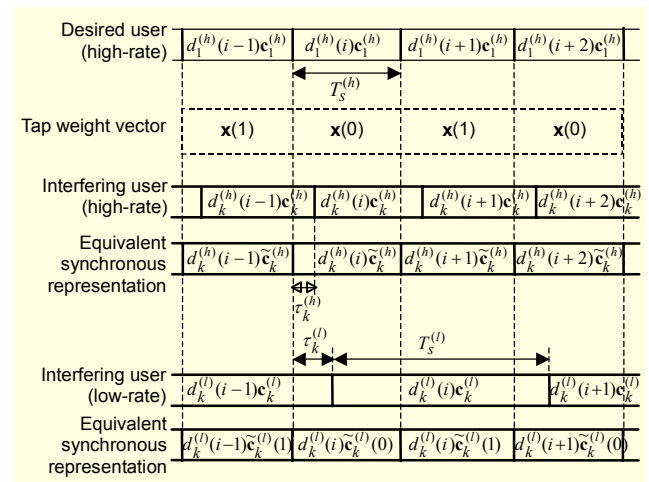


Fig. 2. Example of the relationship between the dual-rate system and the tap weight vector for detecting the desired user when  $m = i \bmod M = 0$ .

#### 1. Interference Cancellation and Demodulation

The output of the proposed adaptive detector for the  $i$ -th bit is

given by

$$z(i) = \mathbf{x}^H(i, m)\mathbf{r}(i), \quad m = 0, \dots, M-1, \quad (9)$$

subject to

$$\mathbf{x}^H(i, m)\mathbf{c}_1^{(h)} = 1, \quad (10)$$

where  $\mathbf{x}(i, m)$  is the tap weight vector, which can be decomposed into adaptive and fixed components, such that

$$\mathbf{x}(i, m) = \mathbf{c}_1^{(h)} - \mathbf{w}^H(i, m), \quad m = i \bmod M, \quad (11)$$

where  $\mathbf{c}_1^{(h)}$  is the fixed component which is the spreading sequence of the desired user and  $\mathbf{w}(i, m)$  is the adaptive component for the  $i$ -th symbol of the desired user in the  $m$ -th interval.

The decision variable for detecting the  $i$ -th bit of the desired user is given as

$$x(i) = \text{Re}[z(i)z^*(i-1)]. \quad (12)$$

For binary DPSK, the bit decision is made by  $\hat{b}_1^{(h)}(i) = \text{sgn}\{x(i)\}$ .

## 2. Modified MMSE Criterion Analysis

The minimization of the following cost function constitutes a modified MMSE criterion:

$$\begin{aligned} J &= E\{|e(i)|^2\} \\ &= E\left\{\left|z(i) \frac{z^*(i-1)}{|z(i-1)|} - \gamma_i d_1^{(h)*}(i) d_1^{(h)}(i-1)\right|^2\right\} \\ &= E\left\{\left|\mathbf{x}^H(m)\mathbf{r}(i) \frac{\mathbf{r}^H(i-1)\mathbf{x}(m')}{|\mathbf{x}(m')\mathbf{r}(i-1)|} - \gamma_i d_1^{(h)*}(i) d_1^{(h)}(i-1)\right|^2\right\}, \quad (13) \end{aligned}$$

subject to

$$\mathbf{x}^H(m)\mathbf{c}_1^{(h)} = \|\mathbf{c}_1^{(h)}\|^2 = 1 \quad \text{for all } m, \quad (14)$$

where  $\gamma_i = \alpha_1^{(h)}(i)[\alpha_1^{(h)*}(i-1)/|\alpha_1^{(h)}(i-1)|]$  is defined as the ratio of the channel coefficients in two consecutive observation intervals. In (13),  $m$  and  $m'$  represent  $i \bmod M$  and  $(i-1) \bmod M$ , respectively.

We next analyze the ability of the time-varying modified MMSE detector to remove the interferences and to provide immunity to the near-far problem.

Expanding (13), we obtain

$$\begin{aligned} J &= E\{e(i)e^*(i)\} \\ &= E\left\{\mathbf{x}^H(m)\mathbf{r}(i) \frac{\mathbf{r}^H(i-1)\mathbf{x}(m')}{|\mathbf{x}(m')\mathbf{r}(i-1)|} \times \frac{\mathbf{x}^H(m')\mathbf{r}(i-1)}{|\mathbf{x}^H(m')\mathbf{r}(i-1)|} \mathbf{r}^H(i)\mathbf{x}(m)\right\} \\ &\quad - E\left\{\gamma_i^* d_1^{(h)*}(i) d_1^{(h)}(i-1) \times \mathbf{x}^H(m)\mathbf{r}(i) \frac{\mathbf{r}^H(i-1)\mathbf{x}(m')}{|\mathbf{x}^H(m')\mathbf{r}(i-1)|}\right\} \\ &\quad - E\left\{\gamma_i d_1^{(h)}(i) d_1^{(h)*}(i-1) \times \frac{\mathbf{x}^H(m')\mathbf{r}(i-1)}{|\mathbf{x}^H(m')\mathbf{r}(i-1)|} \mathbf{r}^H(i)\mathbf{x}(m)\right\} \\ &\quad + E\{|\gamma_i|^2 |d_1^{(h)}(i)|^2 |d_1^{(h)}(i-1)|^2\}, \quad (15) \end{aligned}$$

where the first term of (15) is given by

$$\begin{aligned} &E\left\{\mathbf{x}^H(m)\mathbf{r}(i) \frac{\mathbf{r}^H(i-1)\mathbf{x}(m')}{|\mathbf{x}^H(m')\mathbf{r}(i-1)|} \times \frac{\mathbf{x}^H(m')\mathbf{r}(i-1)}{|\mathbf{x}^H(m')\mathbf{r}(i-1)|} \mathbf{r}^H(i)\mathbf{x}(m)\right\} \\ &= \mathbf{x}^H(m)E\{\mathbf{r}(i)\mathbf{r}^H(i)\mathbf{x}(m)\} \\ &= \mathbf{x}^H(m)\mathbf{R}(i)\mathbf{x}(m) \quad (16) \end{aligned}$$

since

$$\frac{\mathbf{r}^H(i-1)\mathbf{x}(m')}{|\mathbf{x}^H(m')\mathbf{r}(i-1)|} \frac{\mathbf{x}^H(m')\mathbf{r}(i-1)}{|\mathbf{x}^H(m')\mathbf{r}(i-1)|} = 1. \quad (17)$$

Moreover, under the independence assumption of the model in (4), the second term of (15) can be expressed as (18).

$$\begin{aligned} &E\left\{\gamma_i^* d_1^{(h)*}(i) d_1^{(h)}(i-1) \mathbf{x}^H(m)\mathbf{r}(i) \frac{\mathbf{r}^H(i-1)\mathbf{x}(m')}{|\mathbf{x}^H(m')\mathbf{r}(i-1)|}\right\} \\ &= E\left\{\gamma_i^* d_1^{(h)*}(i) d_1^{(h)}(i-1) \times \left[\sum_{k=1}^{K^{(h)}} \sqrt{P_k^{(h)}} d_k^{(h)}(i) \alpha_k^{(h)}(i) \mathbf{x}^H(m) \tilde{\mathbf{c}}_k + \sum_{k=1}^{K^{(l)}} \sqrt{P_k^{(l)}} d_k^{(l)}(i) \alpha_k^{(l)}(i) \mathbf{x}^H(m) \tilde{\mathbf{c}}_k(m)\right]\right. \\ &\quad \left. \times \frac{\sum_{n=1}^{K^{(h)}} \sqrt{P_n^{(h)}} d_n^{(h)*}(i-1) \alpha_n^{(h)*}(i-1) \tilde{\mathbf{c}}_n^{(h)H} \mathbf{x}(m') + \sum_{n=1}^{K^{(l)}} \sqrt{P_n^{(l)}} d_n^{(l)*}(i-1) \alpha_n^{(l)*}(i-1) \tilde{\mathbf{c}}_n^{(l)H}(m') \mathbf{x}(m')}{\left|\sum_{n=1}^{K^{(h)}} \sqrt{P_n^{(h)}} d_n^{(h)}(i-1) \alpha_n^{(h)}(i-1) \mathbf{x}^H(m') \tilde{\mathbf{c}}_n^{(h)} + \sum_{n=1}^{K^{(l)}} \sqrt{P_n^{(l)}} d_n^{(l)}(i-1) \alpha_n^{(l)}(i-1) \mathbf{x}^H(m') \tilde{\mathbf{c}}_n^{(l)}(m')\right|}\right\} \\ &= E\left\{\gamma_i^* d_1^{(h)*}(i) d_1^{(h)}(i-1) d_1^{(h)}(i) \mathbf{x}^H(m) \mathbf{c}_1^{(h)} \times \frac{d_1^{(h)*}(i-1) \alpha_1^{(h)*}(i-1) \mathbf{c}_1^{(h)H} \mathbf{x}(m')}{|d_1^{(h)}(i-1) \alpha_1^{(h)}(i-1) \mathbf{x}^H(m') \mathbf{c}_1^{(h)}|}\right\} \\ &= E\left\{\gamma_i^* |d_1^{(h)*}(i)|^2 |d_1^{(h)}(i-1)|^2 \times \alpha_1^{(h)}(i) \frac{\alpha_1^{(h)*}(i-1)}{|\alpha_1^{(h)}(i-1)|}\right\} \mathbf{x}^H(m) \mathbf{c}_1^{(h)} \mathbf{c}_1^{(h)H} \mathbf{x}(m') \\ &= E\{|\gamma_i|^2\} \mathbf{x}^H(m) \mathbf{c}_1^{(h)} \mathbf{c}_1^{(h)H} \mathbf{x}(m') \\ &= \rho \mathbf{x}^H(m) \mathbf{c}_1^{(h)} \mathbf{c}_1^{(h)H} \mathbf{x}(m'). \quad (18) \end{aligned}$$

In (18), we define  $\rho = E\{|\gamma_i|^2\}$ .

Similarly, the third term of (15) can be obtained as

$$\begin{aligned} & E\left\{\gamma_i d_1^{(h)}(i) d_1^{(h)*}(i-1) \times \frac{\mathbf{x}^H(m') \mathbf{r}(i-1)}{|\mathbf{x}^H(m') \mathbf{r}(i-1)|} \mathbf{r}^H(i) \mathbf{x}(m)\right\} \\ &= E\{|\gamma_i|^2\} \mathbf{x}^H(m') \mathbf{c}_1^{(h)} \mathbf{c}_1^{(h)H} \mathbf{x}(m) \\ &= \rho \mathbf{x}^H(m') \mathbf{c}_1^{(h)} \mathbf{c}_1^{(h)H} \mathbf{x}(m). \end{aligned} \quad (19)$$

The fourth term of (15) can be rewritten as

$$E\{|\gamma_i|^2 |d_1^{(h)}(i)|^2 |d_1^{(h)}(i-1)|^2\} = \rho. \quad (20)$$

We may thus rewrite (15) as

$$\begin{aligned} J &= E\{e(i)e^*(i)\} \\ &= \mathbf{x}^H(m) \mathbf{R}(i) \mathbf{x}(m) - 2\rho \mathbf{x}^H(m) \mathbf{c}_1^{(h)} \mathbf{c}_1^{(h)H} \mathbf{x}(m) + \rho \\ &= \mathbf{x}^H(m) \mathbf{R}(i) \mathbf{x}(m) - \rho \\ &= \mathbf{x}^H(m) [\mathbf{R}_D(i) + \mathbf{R}_{IN}(i)] \mathbf{x}(m) - \rho \\ &= \mathbf{x}^H(m) \mathbf{R}_{IN}(i) \mathbf{x}(m), \end{aligned} \quad (21)$$

where

$$\begin{aligned} \mathbf{R}_D(i) &= E\{D(i)D^H(i)\} \\ &= E\{|\alpha_1^{(h)}(i)|^2\} E\{|d_1^{(h)}(i)|^2\} \mathbf{c}_1^{(h)} \mathbf{c}_1^{(h)H} \\ &= \rho \mathbf{c}_1^{(h)} \mathbf{c}_1^{(h)H} \end{aligned} \quad (22)$$

is the correlation matrix of the desired signal when  $D(i) = \alpha_1^{(h)}(i) d_1^{(h)}(i) \mathbf{c}_1^{(h)}$ , and

$$\mathbf{R}_{IN}(i) = \mathbf{R}(i) - \mathbf{R}_D(i) \quad (23)$$

is the correlation matrix for interference and noise. In the third equality of (22),  $\rho$  can be obtained by

$$\begin{aligned} \rho &= E\{|\gamma_i|^2\} \\ &= E\{\gamma_i \gamma_i^*\} \\ &= E\left\{\alpha_1^{(h)}(i) \frac{\alpha_1^{(h)*}(i-1)}{|\alpha_1^{(h)}(i-1)|} \frac{\alpha_1^{(h)}(i-1)}{|\alpha_1^{(h)}(i-1)|} \alpha_1^{(h)*}(i)\right\} \\ &= E\{\alpha_1^{(h)}(i) \alpha_1^{(h)*}(i)\} \\ &= E\{|\alpha_1^{(h)}(i)|^2\}. \end{aligned} \quad (24)$$

Since minimizing the cost function (21) yields trivial solution  $\mathbf{x}(m) = \mathbf{0}$ , a constraint on the average power of the reference signal to be constant  $\mathbf{x}^H(m) \mathbf{c}_1^{(h)} \mathbf{c}_1^{(h)H} \mathbf{x}(m) = 1$  has been introduced. Then, the new cost function can be rewritten by using Lagrange multiplier  $\lambda$  [15] as

$$\begin{aligned} H &= J - \lambda (\mathbf{x}^H(m) \mathbf{c}_1^{(h)} \mathbf{c}_1^{(h)H} \mathbf{x}(m) - 1) \\ &= \mathbf{x}^H(m) \mathbf{R}_{IN}(i) \mathbf{x}(m) - \lambda (\mathbf{x}^H(m) \mathbf{c}_1^{(h)} \mathbf{c}_1^{(h)H} \mathbf{x}(m) - 1). \end{aligned} \quad (25)$$

We minimize the new cost function  $H$  with respect to the

vector  $\mathbf{x}(m)$ . To do this, we set the derivative  $\partial H / \partial \mathbf{x}^*$  equal to the null vector:

$$\frac{\partial H}{\partial \mathbf{x}^*(m)} = \mathbf{R}_{IN}(i) \mathbf{x}(m) - \lambda \mathbf{c}_1^{(h)} \mathbf{c}_1^{(h)H} \mathbf{x}(m) = \mathbf{0}. \quad (26)$$

Thus,

$$\mathbf{R}_{IN}(i) \mathbf{x}(m) = \lambda \mathbf{c}_1^{(h)} \mathbf{c}_1^{(h)H} \mathbf{x}(m). \quad (27)$$

This means that  $\lambda$  is the eigenvalue of the generalized eigenvector. Substituting (27) into (21), the cost function is given by

$$\begin{aligned} J &= \mathbf{x}^H(m) \mathbf{R}_{IN}(i) \mathbf{x}(m) \\ &= \lambda \mathbf{x}^H(m) \mathbf{c}_1^{(h)} \mathbf{c}_1^{(h)H} \mathbf{x}(m) \\ &= \lambda. \end{aligned} \quad (28)$$

It is clear from (27) and (28) that  $\mathbf{x}(m)$  is an eigenvector and  $\lambda$  is an eigenvalue of the matrix  $\mathbf{R}(i)$ . The eigenvector of  $\mathbf{R}(i)$  that corresponds to the maximum eigenvalue is the vector that minimizes the cost function in (21).

### 3. Adaptive Implementation

Let us consider a DPSK system and assume that the sequence  $b_1^{(h)}(i) = d_1^{(h)}(i) d_1^{(h)*}(i-1)$  is known in training mode and can be estimated in decision-directed mode. The error signal  $e(i)$  is defined as the difference between the detected signal and the compensated desired symbol, that is

$$e(i) = z(i) \frac{z^*(i-1)}{|z(i-1)|} - \hat{\gamma}_i \hat{b}_1^{(h)}(i), \quad (29)$$

where  $\hat{\gamma}_i$  is the estimate of  $\gamma_i = \alpha_1^{(h)}(i) \{\alpha_1^{(h)*}(i-1) / |\alpha_1^{(h)}(i-1)|\}$  in (13), and  $z(i) = \mathbf{x}^H(i, m) \mathbf{r}(i)$ .

#### A. Channel Estimation in a Rayleigh Fading Channel

As shown in Fig. 3, the channel estimation is performed by following an averaging procedure over  $Q$  symbols

$$\hat{\gamma}_i = \hat{\alpha}_1^{(h)}(i) \frac{\hat{\alpha}_1^{(h)*}(i-1)}{|\hat{\alpha}_1^{(h)}(i-1)|}, \quad (30)$$

where

$$\begin{aligned} \hat{\alpha}_1^{(h)}(i) &= \frac{1}{Q} \sum_{q=0}^{Q-1} z(i-q) d_1^{(h)*}(i-q) \\ &= \underbrace{\frac{1}{Q} \sum_{q=0}^{Q-1} \alpha_1^{(h)}(i-q)}_{\hat{\alpha}_1^{(h)}(i)} + \underbrace{\frac{1}{Q} \sum_{q=0}^{Q-1} I(i-q) d_1^{(h)*}(i-q)}_{\hat{\eta}(i)}, \end{aligned} \quad (31)$$

with  $I(i)$  representing the  $i$ -th residual interference and noise.

The variance  $\eta(i)$  is proportional to  $1/Q$ . For a static channel,  $\tilde{\alpha}_1^{(h)}(i)$  equals  $\alpha_1^{(h)}(i)$ , and a large  $Q$  would suppress the noise efficiently. However, a typical mobile radio channel is time-variant, and a large number of averaging periods would lead to a tracking problem with respect to the instantaneous value of  $\alpha_1^{(h)}(i)$ . Therefore, we must find a tradeoff between noise suppression and the tracking of the channel coefficient.

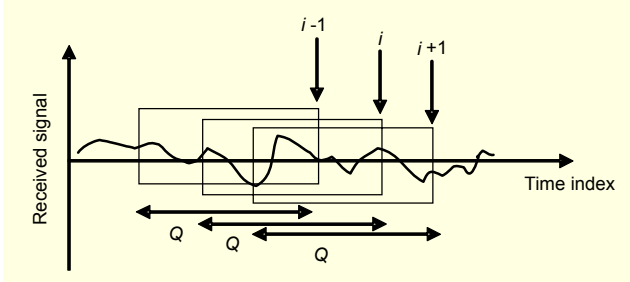


Fig. 3. Relation of channel estimation and time index  $i$ .

### B. Adaptive Algorithm

From (13), the cost function is given by  $Q$  symbols:

$$\begin{aligned} J &= E\{|e(i)|^2\} \\ &= E\{e^*(i)e(i)\} \\ &= E\left\{e^*(i)\left[z(i)\frac{z^*(i-1)}{|z(i-1)|} - \hat{\gamma}_i \hat{b}_1^{(h)}(i)\right]\right\} \\ &= E\left\{e^*(i)\left[\mathbf{x}^H(i,m)\mathbf{r}(i)\frac{\mathbf{r}^H(i-1)\mathbf{x}(i-1,m')}{|\mathbf{x}^H(i-1,m')\mathbf{r}(i-1)|} - \hat{\gamma}_i \hat{b}_1^{(h)}(i)\right]\right\}, \end{aligned} \quad (32)$$

where  $\mathbf{x}(i,m) = \mathbf{c}_1^{(h)} - \mathbf{w}(i,m)$ . The instantaneous estimate of the gradient with respect to  $\mathbf{x}(i,m)$  can be readily obtained by

$$\begin{aligned} \hat{\nabla} J &= -2e^*(i)\frac{\mathbf{r}^H(i-1)\mathbf{x}(i-1,m')}{|\mathbf{x}^H(i-1,m')\mathbf{r}(i-1)|}\mathbf{r}(i) \\ &= -2e^*(i)\frac{z^*(i-1)}{|z(i-1)|}\mathbf{r}(i). \end{aligned} \quad (33)$$

This results in the update equation with period  $M$  for the normalized least mean square (NLMS) algorithm given by

$$\mathbf{w}(i+M,m) = \mathbf{w}(i,m) + \mu(i)\mathbf{r}(i)\frac{z^*(i-1)}{|z(i-1)|}e^*(i), \quad (34)$$

where  $\mu(i)$  is the time-variant step size parameter which is approximated as  $\mu(i) = \tilde{\mu}/\|\mathbf{r}(i)\|^2$ ;  $0 < \tilde{\mu} < 2$  [8], [15].

## IV. Comparison of Differential Detection-Based Adaptive MMSE Detectors

We consider several differential detection-based adaptive MMSE schemes to use as benchmarks for evaluation of the proposed scheme. We summarize the cost functions applied to the adaptive MMSE detectors.

For the time-invariant differential MMSE (TI-differential MMSE) detector [7] incorporated with differential detection, when a one-shot detection is used, the cost function can be equivalently rewritten as

$$\begin{aligned} J &= E\left\{\left|z(i)\frac{z^*(i-1)}{|z(i-1)|} - \hat{b}_1^{(h)}(i)\right|^2\right\}, \quad (35) \\ &\text{subject to } \mathbf{x}^H(i)\mathbf{c}_1^{(h)} = 1, \end{aligned}$$

where  $z(i) = \mathbf{x}^H(i)\mathbf{r}(i)$ .

For the time-invariant modified MMSE (TI-modified MMSE) detector [8] incorporated with differential detection and amplitude compensation, the cost function is given as

$$\begin{aligned} J &= E\left\{\left|z(i)\frac{z^*(i-1)}{|z(i-1)|} - \bar{a}_1^{(h)}(i)\hat{b}_1^{(h)}(i)\right|^2\right\}, \quad (36) \\ &\text{subject to } \mathbf{x}^H(i)\mathbf{c}_1^{(h)} = 1, \end{aligned}$$

where  $z(i) = \mathbf{x}^H(i)\mathbf{r}(i)$ , and  $\bar{a}_1^{(h)}(i)$  is the amplitude estimation for the  $i$ -th bit. It is assumed that the channel coefficients in consecutive intervals are approximately the same:  $\alpha_1^{(h)}(i)[\alpha_1^{(h)*}(i-1)/|\alpha_1^{(h)}(i-1)|] \approx a_1^{(h)}(i)$  when  $\alpha_1^{(h)}(i) = a_1^{(h)}(i)\exp(j\phi_1^{(h)}(i))$ .

For the DMMSE [9], it was assumed that the channel coefficients in two consecutive observation intervals are approximately the same, that is,  $\alpha_1^{(h)}(i) \approx \alpha_1^{(h)}(i-1)$ . The cost function of the DMMSE is given by

$$\begin{aligned} J &= E\{|d_1^{(h)}(i)z(i-1) - d_1^{(h)}(i-1)z(i)|^2\}, \quad (37) \\ &\text{subject to } \mathbf{x}^H(i)\mathbf{R}(i)\mathbf{x}(i) = 1, \end{aligned}$$

where  $z(i) = \mathbf{x}^H(i)\mathbf{r}(i)$ .

For the time-varying differential MMSE (TV-differential MMSE) detector, when the time-varying detection is applied to (35); the cost function can be rewritten as

$$\begin{aligned} J &= E\left\{\left|z(i)\frac{z^*(i-1)}{|z(i-1)|} - \hat{b}_1^{(h)}(i-1)\right|^2\right\}, \quad (38) \\ &\text{subject to } \mathbf{x}^H(i,m)\mathbf{c}_1^{(h)} = 1 \text{ for all } m, \end{aligned}$$

where  $z(i) = \mathbf{x}^H(i,m)\mathbf{r}(i)$ .

When the time-varying modified MMSE (TV-modified



MMSE: proposed scheme) detector is incorporated with differential detection and the ratio of the channel coefficients in two consecutive observation intervals, the cost function is given as (32).

For the time-varying ideal MMSE (TV-ideal MMSE) detector was incorporated with differential detection assuming perfect knowledge of the channel coefficients, the cost function is given as (13).

### 1. Computational Complexity

For a multirate system, using the LMS adaptation, the computational complexity of the time-varying (TV) modified MMSE can be shown to be  $M(8N^{(h)}+2Q+23)$ , where  $M$  is the ratio between high-rate and low-rate. On the other hand, the computational complexity of the time-invariant (TI)-modified MMSE is  $8N^{(h)}+2Q+23$ , while those of the TV-differential MMSE and TI-differential MMSE are  $M(8QN^{(h)}+14)$  and  $8QN^{(h)}+14$ , respectively. When the number of LR users is relatively small, it can be expected that there is little difference in performance between the TI- and TV-modified MMSE since the influence of the channel fluctuation is more serious than that of the LR users. However, as the number of LR users increases, the benefit of the TV-modified MMSE becomes apparent while introducing additional complexity, which is derived in section V.

## V. Simulation Results

In this section, we provide simulation results to verify the performance of the proposed scheme. We first compare the performance of both the time-varying adaptive MMSE (TV-MMSE) and the time-invariant adaptive MMSE (TI-MMSE) [8], [10] detectors under an AWGN channel to verify the TV-MMSE detector's ability to suppress the MAI. Then, dual-rate systems in the presence of fast variation of the channel are considered to compare the performance of the TV-modified MMSE detector with those of the TI-, TV-differential MMSE and TI-modified MMSE detectors. Moreover, the TV-ideal MMSE detector is used to benchmark the evaluation of the proposed scheme.

In the following simulations, we examine an asynchronous dual-rate system, assuming that one-shot detectors are used. Random code sequences with equiprobable  $\pm 1$  elements are used, which satisfy the convergence condition [13], [14]. At the beginning of the simulation, the code sequences are generated and fixed afterward for all trials. A processing gain of 32 is assigned to the HR user, and a processing gain of 64, 128, or 256 is assigned to the LR user. The adaptive MMSE detectors are assumed to be perfectly synchronized to the desired user, while the delays of the interfering users are chosen randomly in

Table 1. Simulation parameters.

Modulation system	DPSK DS/SS
Detection method	Differential detection
Spreading sequences	Random codes (length=32, 64, 128, 256)
$M = T_s^{(l)} / T_s^{(h)}$	2, 4, 8
Transmission channels	Rayleigh fading channel
$f_{\max} T_s^{(h)}$	0.01
$Q$	3

$[0, T_s]$  and the NLMS-type adaptive algorithms are used. For the sake of notational simplicity, we omit the superscript  $(\cdot)$  for the desired user, as in, for example,  $E_b/N_0 = E_b^{(h)}/N_0$ . The near-far ratio,  $NFR_k^{(l)} = P_k^{(l)}/P_1^{(h)}$ , is used to denote the power ratio between the  $k$ -th user and the desired user. In a Rayleigh fading channel, the fading statistics for each user are identical, and the average received signal power is assumed as  $E\{|\alpha_k^{(l)}(i)|^2\} = 1$ . Moreover, the numerical results are obtained by averaging over 500 independent runs. After 2000 iterations, all adaptive detectors reach the steady state. Thus, the adaptive detectors use the same step size  $\tilde{\mu} = 0.05$  and 2000 training bits. The window length (the number of bits) of the channel estimation for the TI- and TV-modified MMSE detectors use  $Q=3$ , since this is the optimum length [8] of averaging intervals when  $f_{\max} T_s^{(h)} = 0.01$ . More detailed parameters used in these simulations are shown in Table 1.

In Fig. 4, we show the BER performance of the TI- and TV-adaptive MMSE detectors versus  $E_b/N_0$  for different values of  $M$ . We can see that the TV-adaptive MMSE detector achieves nearly the same BER performance for all rate ratios. However, the BER performance of the TI-adaptive MMSE detector significantly decreases as the rate ratio  $M$  increases.

To compare the proposed scheme with different differential detection-based schemes, we have investigated the effect of the normalized Doppler frequency and the average  $E_b/N_0$  in a single-rate DS-SS system. Figure 5 compares the average BER performance achieved by five different detectors when the normalized Doppler  $f_{\max} T_s^{(h)}$  varies from 0.002 to 0.2. The BER curve is obtained for  $E_b/N_0 = 40$  dB,  $K=6$  ( $K^{(h)}=6$ ,  $K^{(l)}=0$ ), and  $NFR_k^{(h)} = 15$  dB in a single-rate DS-SS system. As the normalized Doppler frequency increases from 0.01 to 0.2, the BER performance deteriorates remarkably. It would seem that the influence of the Doppler shift is more serious than that of the interference in that region. At  $f_{\max} T_s^{(h)} = 0.02$ , the modified MMSE can achieve a BER of approximately  $10^{-3}$ , while the differential MMSE and the DMMSE [9] fail. These results demonstrate that the modified MMSE detector remarkably

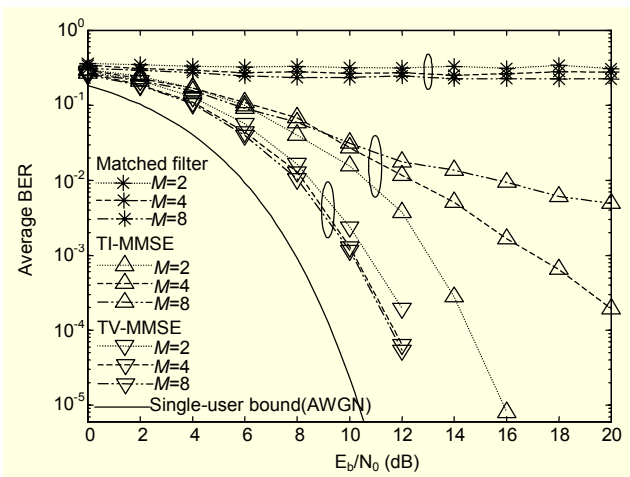


Fig. 4. Average BER as a function of the  $E_b/N_0$  with  $K=8$  ( $K^{(h)}=3$ ,  $K^{(l)}=5$ ),  $NFR_k^{(h)}=NFR_k^{(l)}=10$  dB: dual-rate system in an AWGN channel.

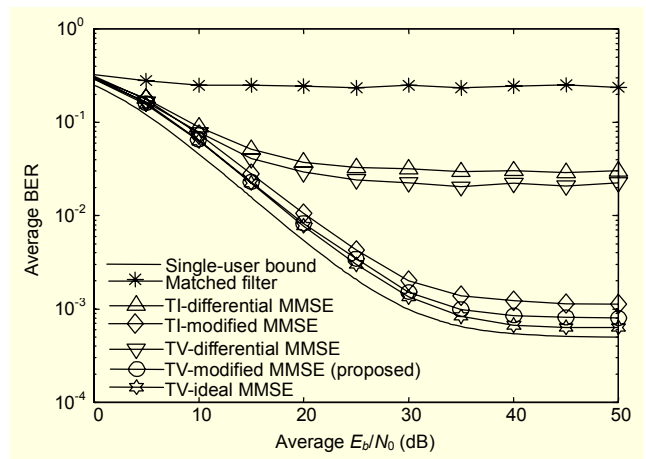


Fig. 7. Average BER as a function of the average  $E_b/N_0$  with  $f_{max}T_s^{(h)}=0.01$ ,  $M=2$ ,  $K=6$  ( $K^{(h)}=3$ ,  $K^{(l)}=3$ ), and  $NFR_k^{(h)}=NFR_k^{(l)}=10$  dB: dual-rate system in a Rayleigh fading channel.

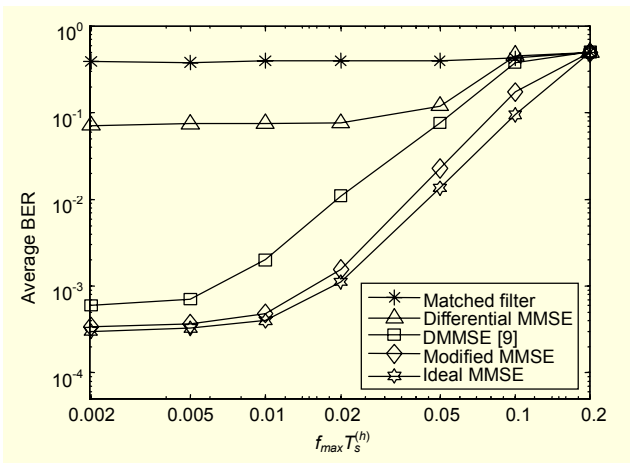


Fig. 5. Average BER as a function of  $f_{max}T_s^{(h)}$  with  $E_b/N_0=40$  dB,  $K=6$  ( $K^{(h)}=6$ ,  $K^{(l)}=0$ ), and  $NFR_k^{(h)}=15$  dB: single-rate system in a Rayleigh fading channel.

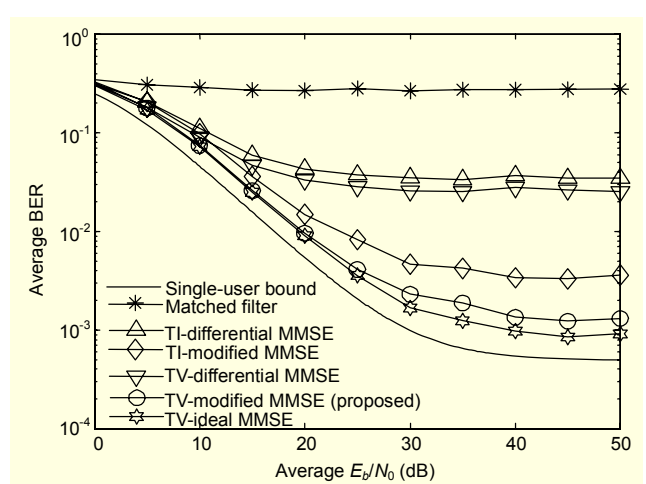


Fig. 8. Average BER as a function of the average  $E_b/N_0$  with  $f_{max}T_s^{(h)}=0.01$ ,  $M=2$ ,  $K=8$  ( $K^{(h)}=3$ ,  $K^{(l)}=5$ ), and  $NFR_k^{(h)}=NFR_k^{(l)}=10$ [dB]: dual-rate system in a Rayleigh fading channel.

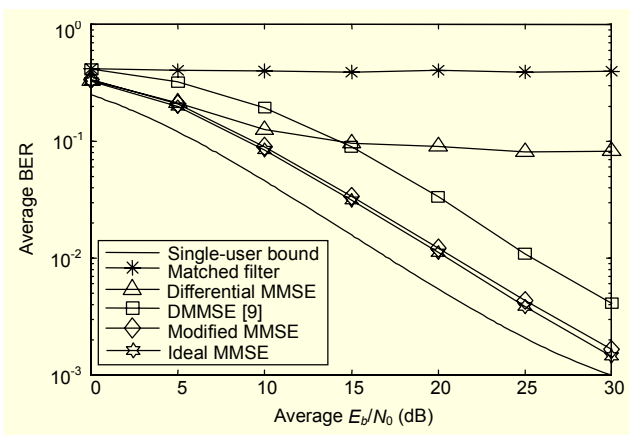


Fig. 6. Average BER as a function of the average  $E_b/N_0$  with  $f_{max}T_s^{(h)}=0.01$ ,  $K=6$  ( $K^{(h)}=6$ ,  $K^{(l)}=0$ ), and  $NFR_k^{(h)}=15$  dB: single-rate system in a Rayleigh fading channel.

outperforms the DMMSE detector for relatively high ranges of the normalized Doppler frequency. It can be inferred from the analysis and simulation results that the modified MMSE is less sensitive to the Doppler shift than the DMMSE.

Figure 6 shows the average BER performance of the detectors as a function of the average  $E_b/N_0$  with  $f_{max}T_s^{(h)}=0.01$ ,  $K=6$  ( $K^{(h)}=6$ ,  $K^{(l)}=0$ ), and  $NFR_s^{(h)}=15$  dB. The results indicate that the modified MMSE is more robust than the DMMSE to strong MAI. In particular, the differential MMSE maintains the error floor at higher  $E_b/N_0$ . It seems that the differential MMSE cannot sufficiently suppress strong MAI caused by the near-far problem.

The BER performance versus the average received  $E_b/N_0$  is



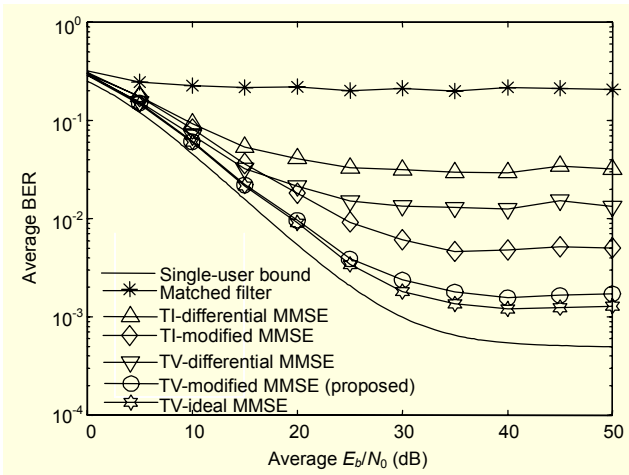


Fig. 9. Average BER as a function of the average  $E_b/N_0$  with  $f_{\max} T_s^{(h)}=0.01$ ,  $M=4$ ,  $K=6$  ( $K^{(h)}=3$ ,  $K^{(l)}=3$ ), and  $NFR_k^{(h)}=NFR_k^{(l)}=10$  dB: dual-rate system in a Rayleigh fading channel.

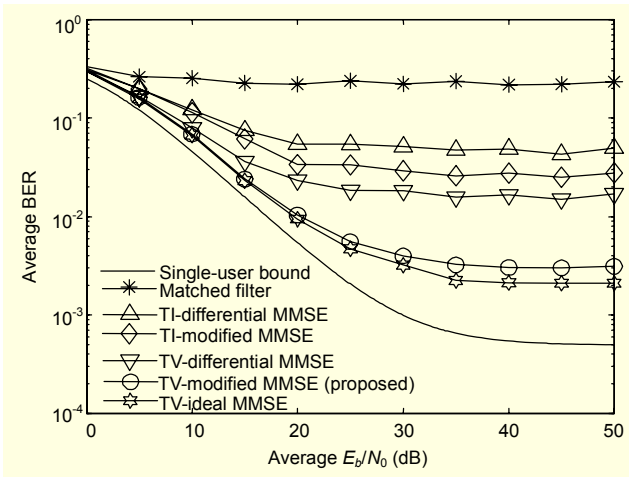


Fig. 10. Average BER as a function of the average  $E_b/N_0$  with  $f_{\max} T_s^{(h)}=0.01$ ,  $M=4$ ,  $K=8$  ( $K^{(h)}=3$ ,  $K^{(l)}=5$ ), and  $NFR_k^{(h)}=NFR_k^{(l)}=10$  dB: dual-rate system in a Rayleigh fading channel.

shown in Figs. 7 and 8. We have simulated a system where the HR and LR users' spreading gains are 32 and 64 respectively. It is seen that the TI-, TV-modified, and TV-ideal MMSE detectors clearly outperform the others. In Fig. 7, the modified MMSE offers significantly better performance than the differential MMSE, but there is little difference in performance between the TI- and TV-modified MMSE. This is because the influence of channel fluctuation is more serious than that of the LR users. However, as the number of LR users increases, the benefit of the TV-modified MMSE becomes apparent as shown in Fig. 8.

In Figs. 9 and 10, we plot the BER performance as a function of the average received  $E_b/N_0$  when  $K=6$  ( $K^{(h)}=3$ ,

$K^{(l)}=3$ ) and  $K=8$  ( $K^{(h)}=3$ ,  $K^{(l)}=5$ ), respectively. We have simulated a system where the HR and LR users' spreading gains are 32 and 128 respectively. When we compare the performance of the TI-MMSE detectors with those of the TV-MMSE detectors, we can see that the performance of the TI-MMSE detectors deteriorates significantly because the cross correlations between different users' spreading sequences change from symbol to symbol for the HR user in multirate systems.

Figures 7 to 10 demonstrate that the TI-modified MMSE using differential detection and channel compensation can improve performance significantly when compared to single differential detection. Also, as the number of LR users increases, further performance improvement is obtained by applying time-varying detection, while introducing additional complexity. Moreover, as  $M$  increases, the time-invariant schemes deteriorate significantly.

## VI. Conclusion

In this paper, we have proposed a time-varying modified MMSE detector for multirate CDMA systems in the presence of fast channel variation. This scheme can compensate fast channel variation inherently, thus the detector can effectively suppress the MAI in fast Rayleigh fading channels. As shown by analytic and numerical results, the TI-MMSE detector incurs a large loss in BER performance when compared to the TV-MMSE detector. The TV-modified MMSE detector is more robust to strong MAI caused by the near-far problem than the TI-modified MMSE. Furthermore, the TV-modified MMSE detector for the HR user achieves a lower BER performance when compared to other TI- and TV-MMSE detectors.

## References

- [1] E. Dahlman, E. Gudmundson, M. Nilsson, and J. Skold, "UMTS/IMT-2000 Based on Wideband CDMA," *IEEE Commun. Mag.*, vol. 36, no. 9, Sep. 1998, pp. 70-80.
- [2] P. Taaghoul, B.G. Evans, E. Buracchini, R. De Gaudenzi, G. Gallinaro, J.H. Lee, and C.G. Kang, "Satellite UMTS/IMT-2000 W-CDMA Air Interfaces," *IEEE Commun. Mag.*, vol. 37, no. 9, Sep. 1999, pp. 116-126.
- [3] U. Mitra, "Comparison of Maximum Likelihood-Based Detection for Two Multi-Rate Access Schemes for CDMA Signals," *IEEE Trans. Commun.*, vol. 47, no. 1, Jan. 1999, pp. 64-77.
- [4] J. Chen and U. Mitra, "Analysis of Decorrelator-Based Receivers for Multirate DS/CDMA Communications," *IEEE Trans. Veh. Technol.*, vol. 48, no. 6, Nov. 1999, pp. 1966-1983.

- [5] S. Buzzi, M. Lops, and A.M. Tulino, "Blind Adaptive Multiuser Detection for Asynchronous Dual-Rate DS/CDMA Systems," *IEEE J. Select. Areas Commun.*, vol. 19, no. 2, Feb. 2001, pp. 233-244.
- [6] A. Sabharwal, U. Mitra, and R. Moses, "MMSE Receivers for Multirate DS-CDMA Systems," *IEEE Trans. Commun.*, vol. 49, no. 12, Dec. 2001, pp. 2184-2197.
- [7] S. Yoshida, A. Ushirokawa, S. Yanagi, and Y. Furuya, "DS/CDMA Adaptive Interference Canceller on Differential Detection for Fast Fading Channel," *Proc. 44th Vehicular Technology Conference*, June 1994, pp. 780-784.
- [8] K.S. Jeong, M. Yokoyama, and H. Uehara, "Performance Improvement of MAI Cancellation in Fading DS/CDMA Channels," *IEICE Trans. Fundamentals*, vol. E88-A, no. 10, Oct. 2005, pp. 2869-2877.
- [9] U. Madhow, K. Bruvold, and L.J. Zhu, "Differential MMSE: A Framework for Robust Adaptive Interference Suppression for DS-CDMA over Fading Channels," *IEEE Trans. Commun.*, vol. 53, no. 8, Aug. 2005, pp. 1377-1390.
- [10] M. Honig, U. Madhow, and S. Verdu, "Blind Adaptive Multiuser Detection," *IEEE Trans. Inform. Theory*, vol. 41, no. 4, July 1995, pp. 944-960.
- [11] A.N. Barbosa and S.L. Miller, "Adaptive Detection of DS/CDMA Signals in Fading Channels," *IEEE Trans. Commun.*, vol. 46, no. 1, Jan. 1998, pp. 115-124.
- [12] M. Latva-aho and M. Juntti, "LMMSE Detection for DS-CDMA Systems in Fading Channels," *IEEE Trans. Commun.*, vol. 48, no. 2, Feb. 2000, pp. 194-199.
- [13] J. Chen and U. Mitra, "Optimum Near-Far Resistance for Dual-Rate DS/CDMA Signals: Random Signature Sequence Analysis," *IEEE Trans. Inform. Theory*, vol. 45, Nov. 1999, pp. 2434-2447.
- [14] H. Yan and S. Roy, "Parallel Interference Cancellation for Uplink Multirate Overlay CDMA Channels," *IEEE Trans. Commun.*, vol. 53, no. 1, Jan. 2005, pp. 152-161.
- [15] S. Haykin, *Adaptive Filter Theory*, Prentice Hall, 1996.
- [16] J.G. Proakis, *Digital Communications*, 3rd ed., McGraw-Hill, 1995.



**Kilsso Jeong** received the BE degree in electronic engineering from Yeungnam University, Korea, in 1999, and the ME degree in information and computer sciences engineering from Toyohashi University of Technology, Toyohashi, Japan, in 2003.

Currently, he is in the PhD program in the Department of Information and Computer Sciences at Toyohashi University of Technology. His research interests include channel estimation and interference cancellation techniques for wireless communication systems. He is a Student Member of the IEEE and IEICE.



**Mitsuo Yokoyama** received the BE and DE degrees in communications engineering from Tohoku University, Sendai, Japan, in 1964 and 1981, respectively. He joined the Communications Research Laboratory, Ministry of Posts and Telecommunications in 1964, where he was engaged in research on

satellite communications, land mobile digital communications, and multi-media communications, including wired and radio communications. He moved to Toyohashi University of Technology in 1996, where he is currently a Professor at the Department of Information and Computer Sciences. His current research interests include mobile communication techniques and self-organizing mobile networks. He received the Science and Technology Agency Chief Prize in 1989, and the Ministry of Posts and Telecommunications Minister Commendation in 1994. He has written several books on spread spectrum techniques, mobile communications, and mobile networks. Dr. Yokoyama is a Member of IEEE and IEIJ.



**Hideyuki Uehara** received the BE, ME, and PhD degrees in electrical engineering from Keio University, Yokohama, Japan, in 1992, 1994, and 1997, respectively. Since 1997, he has been with the Department of Information and Computer Sciences, Toyohashi University of Technology, Japan, where he is now an

Associate Professor. From 2002 to 2003, he was also a Visiting Researcher at the Advanced Telecommunications Research Institute International (ATR), Kyoto, Japan. His current research interests include wireless networks, mobile communication systems, optical communication systems, and information theory. Dr. Uehara is a Member of IEEE, ACM, IPSJ, and SITA.